NIFS--89

JP9109092

Nonlinear Behavior of Multiple-Helicity Resistive Interchange Modes near Marginally Stable States

H. Sugama, N. Nakajima and M. Wakatani

(Received – May 1, 1991)

NIFS-89 May 1991

Nonlinear behavior of multiple-helicity resistive interchange modes near marginally stable states

Hideo Sugama and Noriyoshi Nakajima
National Institute for Fusion Science, Nagoya 464-01, Japan
Masahiro Wakatani
Plasma Physics Laboratory, Kyoto University, Uji 611, Japan

ABSTRACT

Nonlinear behavior of resistive interchange modes near marginally stable states is theoretically studied under the multiple-helicity condition. Reduced fluid equations in the sheared slab configuration are used in order to treat a local transport problem. With the use of the invariance property of local reduced fluid model equations under a transformation between the modes with different rational surfaces, weakly nonlinear theories for single-helicity modes by Hamaguchi [Phys. Fluids B **1**, 1416 (1989)] and Nakajima [Phys. Fluids B **2**, 1170 (1990)] are extended to the multiple-helicity case and applied to the resistive interchange modes. We derive the nonlinear amplitude equations of the multiple-helicity modes, from which the convective transport in the saturated state is obtained. It is shown how the convective transport is enhanced by nonlinear interaction between modes with different rational surfaces compared with the single-helicity case. We confirm that theoretical results are in good agreement with direct numerical simulations.

KEYWORDS: resistive interchange mode, weakly nonlinear theory, multiple-helicity, anomalous transport, reduced MHD model

I. INTRODUCTION

In magnetically confined plasmas inhomogeneities of magnetic fields, currents, pressure, density and temperature cause a variety of instability to grow and have finite amplitudes for which linear theory is no longer valid. A lot of phenomena in plasmas such as sawtooth oscillations, disruptions in tokamaks and self-reversal of magnetic fields in RFP plasmas are considered as essentially nonlinear processes. Another important example of nonlinear phenomena is anomalous transport[1] which is observed in most of magnetically confinement systems and is considered to be the enhancement of transport due to fluctuations or turbulence in plasmas. Generally such nonlinear problems are complex and especially theoretical quantitative treatment of strong nonlinear or turbulent systems is still difficult so that complete understanding of anomalous transport as strongly nonlinear processes is *not* yet achieved. However weakly nonlinear theories,[2] which treat nonlinear interaction of the modes with small amplitudes, have been developed and applied successfully to some problems of fluid mechanics and plasma physics.

Landau presented a weakly nonlinear theory based on a general model and described bifurcation of the system from one steady state to another using his model equation called the Landau equation.[3] Palm derived the Landau equation from the partial differential equations describing the system for a problem of Bénard convection.[4] Malkus, Veronis and many authors applied a weakly nonlinear theory to problems of hydrodynamic stability.[2,5] Also based on plasma fluid models, Hamaguchi and Nakajima developed a weakly nonlinear theory for single-helicity modes of plasma instabilites.[6–8] They derived some parameter dependence of the amplitude of the steady nonlinear solution and the convective transport theoretically. These weakly nonlinear theories allow us quantitative and partially analytical treatment of nonlinear behavior of the system near the marginally stable state and give us some clues to the understanding of properties in the strongly nonlinear regime and anomalous transport.

In this paper we will develop the weakly nonlinear theory for resistive interchange modes with multiple-helicity. A single-helicity condition gives a two-dimensional problem in which

nonlinear interaction only among the modes localized around the same rational surface is treated while we must consider also nonlinear interaction among the modes with different rational surfaces in the multiple-helicity case which is essentially three-dimensional. When we are concerned with plasma transport in the sheared magnetic fields, it is natural to include the contributions from all linearly unstable modes lying at different radial positions rather than from only modes localized around a single surface and necessarily we must consider the multiple-helicity problem. Generally multiple-helicity or three-dimensional problems are complex although it will be shown that the weakly nonlinear theory for the single-helicity modes is easily generalized to the multiple-helicity case by noting the invariance property of the fluid model equations under a certain transformation of the multiple-helicity modes. We will find that this property holds for many kinds of reduced fluid model equations based on the local sheared slab geometry which is often assumed *for local transport problems*. The equations governing the amplitudes of the multiple-helicity resistive interchange modes will be derived. Due to the invariance property of the local fluid model equations, they have symmetric solutions which are also invariant under the transformation of the multiple-helicity modes. The symmetric solutions consist of a virtually infinite sequence of mutiple-helicity modes with the same radial structure localized around their own rational surfaces, which are similar to the structure of ballooning modes.[9] Using these symmetric solutions is more relevant for local description of the system (which is analogous to the eikonal representation in geometrical optics) than using bounded solutions which vanishes at some boundaries and are confined within the finite radial region. For the symmetric solutions, the amplitude equations reduce to the Landau equation, for which we have a simple analytical expression of the solutions.

The resistive interchange modes are considered to be linearly unstable in the peripheral region of stellarator/heliotron plasmas which have a magnetic hill there and therefore they are *candidates* for the cause of edge turbulence and anomalous transport.[6,10~13] Convective transport in the nonlinearly saturated states of multiple-helicity resistive interchange modes near marginally stable states will be studied by using the weakly nonlinear theory and comparison between theoretical results and those obtained by direct numerical simulation

will be shown. We will find how transport is changed by the effects of nonlinear interaction of modes with different rational surfaces compared with the single-helicity case.

This paper is organized as follows. In Sec.II the fluid model equations describing the resistive interchange modes is explained. In Sec.III we find general symmetry properties of reduced fluid equations based on the local sheared slab configuration. In Sec.IV we develop the weakly nonlinear theory for the multiple-helicity resistive interchange modes and derive the equations governing the amplitudes of multiple-helicity modes. In Sec.V symmetric solutions of the amplitude equations are given and convective transport in the nonlineary saturated states is obtained. The effects of multiple-helicity on transport are investigated and theoretical results are compared with numerical simulation results. Finally conclusions and discussion are given in Sec.VI.

II. MODEL EQUATIONS

Resistive interchange modes are described by the following reduced MHD model[6,10–12,14] in the electrostatic limit, which consists of the vorticity equation:

$$\frac{\rho_m c}{B_0}\left(\frac{\partial}{\partial t}-\nu\nabla_\perp^2+\frac{c}{B_0}\hat{z}\times\nabla\phi\cdot\nabla\right)\nabla_\perp^2\phi=-\frac{B_0}{c\eta}\nabla_\parallel^2\phi-\Omega'\frac{\partial p}{\partial y} \tag{1}$$

and the pressure convection equation:

$$\left(\frac{\partial}{\partial t}-\chi\nabla_\perp^2+\frac{c}{B_0}\hat{z}\times\nabla\phi\cdot\nabla\right)p=\frac{c}{B_0}P_0'\frac{\partial\phi}{\partial y} \tag{2}$$

where ϕ is the electrostatic potential, p the pressure fluctuation, B_0 the component of the static magnetic field along the z-axis, ρ_m the average mass density, c the light velocity in the vacuum, η the resistivity, ν the kinematic viscosity, χ the pressure diffusivity, $P_0' \equiv dP_0/dx$ (<0) the volume-averaged pressure gradient and $\Omega' \equiv d\Omega/dx$ (>0) the average curvature of the magnetic field line. $\nabla_\perp^2=\partial_x^2+\partial_y^2$ denotes the two-dimensional Laplacian. The gradient along the the static sheared magnetic field line is given by

$$\nabla_\parallel=\frac{\partial}{\partial z}+\frac{x}{L_s}\frac{\partial}{\partial y}. \tag{3}$$

Here B_0, L_s, ρ_m, η, ν, χ, P_0' and Ω' are assumed to be constant since we treat a local transport problem. The electrostatic approximation is used in Eqs.(1) and (2) since we consider the low beta plasma in the peripheral region.

Choosing the units:

$$\begin{aligned}
&[t]=(-P_0'\Omega'/\rho_m)^{-1/2} \qquad && [x]=[y]=cL_s\eta^{1/2}(-\rho_m P_0'\Omega')^{1/4}/B_0\\
&[z]=L_s && [\chi]=[x]^2/[t]=c^2\eta(-P_0')\Omega' L_s^2/B_0^2\\
&[\phi]=c\eta(-P_0')\Omega' L_s^2/B_0 && [p]=cL_s\eta^{1/2}\rho_m^{1/4}(-P_0')^{5/4}\Omega'^{1/4}/B_0
\end{aligned} \tag{4}$$

we obtain model equations in non-dimensional variables from Eqs.(1) and (2) as follows

$$\partial_t\nabla_\perp^2\phi+[\phi,\nabla_\perp^2\phi] = -\nabla_\parallel^2\phi-\partial_y p+\chi P_r\nabla_\perp^4\phi \tag{5}$$

$$\partial_t p+[\phi,p] = -\partial_y\phi+\chi\nabla_\perp^2 p \tag{6}$$

where

$$\nabla_\parallel=\partial_z+x\partial_y. \tag{7}$$

The Prandtl number is defined by

$$P_r = \nu/\chi. \tag{8}$$

All the nonlinear terms appear in the form of Poisson brackets:

$$[f, g] = (\partial_x f)(\partial_y g) - (\partial_x g)(\partial_y f). \tag{9}$$

III. SYMMETRY PROPERTY OF LOCAL SLAB MODEL WITH CONSTANT MAGNETIC SHEAR

Here we discuss the symmetry property of the local model equations (5) and (6). The electrostatic potential ϕ and the pressure fluctuation p are expanded into the Fourier series with respect to y and z as

$$\begin{aligned}\begin{pmatrix}\phi(x,y,z)\\ p(x,y,z)\end{pmatrix} &= \sum_{m=-\infty}^{\infty}\sum_{n=-\infty}^{\infty}\begin{pmatrix}\phi_{mn}(x)\\ p_{mn}(x)\end{pmatrix}\exp 2\pi i(my/L_y+nz/L_z)\\ &= \sum_{m=-\infty}^{\infty}\sum_{n=-\infty}^{\infty}\begin{pmatrix}\phi_{mn}(x)\\ p_{mn}(x)\end{pmatrix}\exp ik(my+n\Delta z)\end{aligned} \tag{10}$$

where L_y and L_z are the maximum scale lengths of the fluctuations in the y and z directions, respectively, and we defined

$$k \equiv 2\pi/L_y, \qquad \Delta \equiv L_y/L_z. \tag{11}$$

The wavenumbers of the Fourier modes in the y and z directions are given by $k_y \equiv 2\pi m/L_y = mk$ and $k_z \equiv 2\pi n/L_y = nk\Delta$, respectively, where $m,n = 0,\pm1,\pm2,\cdots$ are the mode numbers. Here $k \equiv 2\pi/L_y$ denotes the minimum wavenumber of the fluctuations in the y direction.

We consider the following functional transformation $\mathbf{T}$:

$$\mathbf{T}:\begin{pmatrix}\phi(x,y,z)\\ p(x,y,z)\end{pmatrix}\to\begin{pmatrix}(T\phi)(x,y,z)\\ (Tp)(x,y,z)\end{pmatrix}=\begin{pmatrix}\phi(x-\Delta,y-\Delta z,z)\\ p(x-\Delta,y-\Delta z,z)\end{pmatrix} \tag{12}$$

which is expressed in terms of the Fourier mode as

$$\mathbf{T}:\begin{pmatrix}\phi_{m,n}(x)\\ p_{m,n}(x)\end{pmatrix}\to\begin{pmatrix}(T\phi)_{m,n}(x)\\ (Tp)_{m,n}(x)\end{pmatrix}=\begin{pmatrix}\phi_{m,m+n}(x-\Delta)\\ p_{m,m+n}(x-\Delta)\end{pmatrix}. \tag{13}$$

For arbitrary functions $f(x,y,z)$ and $g(x,y,z)$, we have

$$\left.\begin{aligned}&\partial_x Tf = T\partial_x f, \qquad \partial_y Tf = T\partial_y f\\ &[Tf,Tg] = T[f,g], \quad \nabla_\parallel Tf = T\nabla_\parallel f\end{aligned}\right\} \tag{14}$$

Defining

$$\mathbf{\Phi} = \begin{pmatrix} \phi \\ p \end{pmatrix}, \qquad \mathbf{A} = \begin{pmatrix} \nabla_\perp^2 & 0 \\ 0 & 1 \end{pmatrix}$$

$$\mathbf{F}[\mathbf{\Phi}] = \begin{pmatrix} -\nabla_\parallel^2 \phi - \partial_y p + \chi P_r \nabla_\perp^4 \phi - [\phi, \nabla_\perp^2 \phi] \\ -\partial_y \phi + \chi \nabla_\perp^2 \phi - [\phi, p] \end{pmatrix} \tag{15}$$

Eqs.(5) and (6) are rewritten as

$$\partial_t \mathbf{A}\mathbf{\Phi} = \mathbf{F}[\mathbf{\Phi}] \tag{16}$$

We find from Eqs.(14) that $\mathbf{T}$ commutes with $\mathbf{A}$ and $\mathbf{F}$

$$\mathbf{AT} = \mathbf{TA}, \quad \mathbf{FT} = \mathbf{TF} \tag{17}$$

Thus it follows that Eq.(14) is invariant with the transformation $\mathbf{T}$, i.e., for an arbitrary solution $\mathbf{\Phi}$ of Eq.(16), $\mathbf{T\Phi} \equiv (T\Phi, Tp)^T$ is also *the solution*

$$\partial_t \mathbf{A}[\mathbf{T\Phi}] = \mathbf{F}[\mathbf{T\Phi}]. \tag{18}$$

We should note that not only Eqs.(5) and (6) but also other reduced fluid model equations based on the local sheared slab geometry with constant magnetic shear are invariant under the transformation $\mathbf{T}$.

Next we define another functional transformation $\mathbf{P}$:

$$\mathbf{P} : \begin{pmatrix} \phi(x, y, z) \\ p(x, y, z) \end{pmatrix} \to \begin{pmatrix} -\phi(x, -y, -z) \\ p(x, -y, -z) \end{pmatrix} \tag{19}$$

which is expressed in terms of the Fourier mode as

$$\mathbf{P} : \begin{pmatrix} \phi_{m,n}(x) \\ p_{m,n}(x) \end{pmatrix} \to \begin{pmatrix} -\phi_{-m,-n}(x) \\ p_{-m,-n}(x) \end{pmatrix} = \begin{pmatrix} -\phi^*_{m,n}(x) \\ p^*_{m,n}(x) \end{pmatrix} \tag{20}$$

where a superscript $*$ denotes a complex conjugate. Here we used the reality of the values of the functions $\phi(x, y, z)$ and $p(x, y, z)$, which yields

$$\phi^*_{m,n}(x) = \phi_{-m,-n}(x), \quad p^*_{m,n}(x) = p_{-m,-n}(x). \tag{21}$$

Equations (5) and (6) (or Eq.(16)) are invariant with the transformation $\mathbf{P}$, i.e., Eq.(16) gives

$$\partial_t \mathbf{A}[\mathbf{P\Phi}] = \mathbf{F}[\mathbf{P\Phi}]. \tag{22}$$

It should be remarked that this invariance under the transformation $\mathbf{P}$ results from the fact that Eqs.(5) and (6) are derived from the one-fluid MHD model.[12,15] Therefore this invariance is broken for the two-fluid type model equations which include the electron or ion diamagnetic effects. From the invariance property, we can assume the solution of Eqs.(5) and (6) (or Eq.(16)) satisfying

$$\mathbf{P\Phi} = \mathbf{\Phi} \tag{23}$$

which is valid at any time t if it is at the initial time $t = 0$. Then the solution Φ satisfying Eq.(23) is expanded into the Fourier series as

$$\begin{pmatrix} \phi(x,y,z) \\ p(x,y,z) \end{pmatrix} = \sum_{n=0}^{\infty} \begin{pmatrix} \phi_{0n}(x)\sin kn\Delta z \\ p_{0n}(x)\cos kn\Delta z \end{pmatrix} + \sum_{m=1}^{\infty}\sum_{n=-\infty}^{\infty} \begin{pmatrix} \phi_{mn}(x)\sin k(my+n\Delta z) \\ p_{mn}(x)\cos k(my+n\Delta z) \end{pmatrix}, \tag{24}$$

where $\phi_{mn}(x)$ and $p_{mn}(x)$ are the real-valued functions which are transformed by $\mathbf{T}$ in the same manner as in Eq.(13).

IV. WEAKLY NONLINEAR THEORY OF MULTIPLE-HELICITY RESISTIVE INTERCHANGE MODES

Here we treat the resistive interchange modes near the marginal stable states by the weakly nonlinear theory. Equations (5) and (6) have the trivial equilibrium solution $\phi = p = 0$. Solving the linearized equation gives the spectrum of the eigenvalue or the linear growth rate γ for the perturbaton which varies in the form $\exp \gamma t$ and vanishes as $x \to \pm\infty$. When the Prandtl number P_τ is fixed, a critical diffusivity χ_c exists such that all the Fourier modes in Eq.(24) are linearly stable for $\chi > \chi_c$, only one of the eigenvalues of the $m = 1$ modes becomes $\gamma = 0$ for $\chi = \chi_c$ and the system is linearly unstable for $\chi < \chi_c$. Since the neighborhood of the marginally stable states $\chi = \chi_c$ is considered, the magnitudes and the temporal variations of $\phi(x, y, z)$ and $p(x, y, z)$ are small and therefore we make the following perturbation expansion with the parameter λ

$$\begin{aligned}
\begin{pmatrix} \phi \\ p \end{pmatrix} &= \lambda \begin{pmatrix} \phi_1 \\ p_1 \end{pmatrix} + \lambda^2 \begin{pmatrix} \phi_2 \\ p_2 \end{pmatrix} + \cdots\cdots \\
\frac{\partial}{\partial t} &= \lambda \frac{\partial}{\partial \tau_1} + \lambda^2 \frac{\partial}{\partial \tau_2} + \cdots\cdots \\
\chi &= \chi_c + \lambda \chi_1 + \lambda^2 \chi_2 + \cdots\cdots .
\end{aligned} \tag{25}$$

Substituting Eq.(25) into Eqs.(5) and (6) yields in $O(\lambda)$

$$\mathbf{L} \begin{pmatrix} \phi_1 \\ p_1 \end{pmatrix} \equiv \begin{pmatrix} -\nabla_{\parallel}^2 \phi_1 + \chi_c P_\tau \nabla_\perp^4 \phi_1 & -\partial_y p_1 \\ \partial_y \phi_1 & -\chi_c \nabla_\perp^2 p_1 \end{pmatrix} = 0. \tag{26}$$

Equation (26) is just the linear equation for the marginally stable state. As stated above the solution of Eq.(26) consists of the linear combination of the $m = 1$ modes

$$\begin{pmatrix} \phi_1 \\ p_1 \end{pmatrix} = \sum_{n=-\infty}^{\infty} A_n \begin{pmatrix} \phi_1(x + n\Delta) \sin k(y + n\Delta z) \\ p_1(x + n\Delta) \cos k(y + n\Delta z) \end{pmatrix}. \tag{27}$$

Here we used the fact that since the linear equation (26) is also invariant with the transformation $\mathbf{T}$, we can produce the linear solutions from one set of eigenfunctions $(\phi_1(x) \sin ky$,

$p_1(x)\cos ky)^T$ by operating $\mathbf{T}$ successively

$$\mathrm{T}^n \begin{pmatrix} \phi_1(x)\sin ky \\ p_1(x)\cos ky \end{pmatrix} = \begin{pmatrix} \phi_1(x-n\Delta)\sin k(y-n\Delta z) \\ p_1(x-n\Delta)\cos k(y-n\Delta z) \end{pmatrix} \qquad (n=0,\pm1,\pm2,\cdots). \tag{28}$$

Thus the marginally stable state is degenerate with the m=1 mode eigenfunctions (28). Here we employ the boundary condition that $\phi(x) \to 0$ as $x \to \infty$. The eigenfunction $\phi(x)$ has a peak at $x = 0$ so that the m=1 modes (28) are localized around the mode rational surfaces $x = n\Delta$ $(n = 0, \pm1, \pm2, \cdots)$. In Eq.(27) A_n is a real-valued function of the time:

$$A_n = A_n(\tau_1, \tau_2, \cdots). \tag{29}$$

When the linear operator $\mathbf{L}$ defined by Eq.(26) acts on the (m,n) Fourier mode in Eq.(24), it is replaced with $\mathbf{L}_{mn}$ given by

$$\mathbf{L}_{mn} \equiv \begin{pmatrix} m^2k^2(x+\frac{n}{m}\Delta)^2 + \chi_c P_r(\partial_x^2 - m^2k^2)^2 & mk \\ mk & -\chi_c(\partial_x^2 - m^2k^2) \end{pmatrix}. \tag{30}$$

For arbitrary function vectors $\boldsymbol{u} = (u_1(x), u_2(x))^T$ and $\boldsymbol{v} = (v_1(x), v_2(x))^T$, the inner product is defined by

$$\langle \boldsymbol{u}, \boldsymbol{v} \rangle \equiv \int_{-\infty}^{\infty} dx \{u_1(x)v_1(x) + u_2(x)v_2(x)\} \tag{31}$$

We see from Eq.(30) that the linear operator $\mathbf{L}_{mn}$ is self-adjoint with respect to the inner bracket (31), i.e.,

$$\langle \boldsymbol{u}, \mathbf{L}_{mn}\boldsymbol{v} \rangle = \langle \mathbf{L}_{mn}\boldsymbol{u}, \boldsymbol{v} \rangle. \tag{32}$$

Equation (26) is rewritten by using Eq.(30) as

$$L_{1n} \begin{pmatrix} \phi_1(x+n\Delta) \\ p_1(x+n\Delta) \end{pmatrix} \equiv \begin{pmatrix} k^2(x+n\Delta)^2 + \chi_c P_r(\partial_x^2 - k^2)^2 & k \\ k & -\chi_c(\partial_x^2 - k^2) \end{pmatrix} \begin{pmatrix} \phi_1(x+n\Delta) \\ p_1(x+n\Delta) \end{pmatrix} = 0 \tag{33}$$

which gives the profiles of the eigenfunctions $\phi_1(x)$ and $p_1(x)$, however, does not determine the mode amplitude A_n. For the mode number $m \geq 2$, the linear groth rates are negative and $\mathbf{L}_{mn}$ is invertible so that $\mathbf{L}_{mn}\boldsymbol{u} = 0$ gives the trivial solution $\boldsymbol{u} = 0$.

Equations (5) and (6) yield in $O(\lambda^2)$

$$\mathbf{L}\begin{pmatrix}\phi_2\\ p_2\end{pmatrix}=\begin{pmatrix}\partial_{\tau_1}\nabla_\perp^2\phi_1-\chi_1 P_r\nabla_\perp^4\phi_1+[\phi_1,\nabla_\perp^2\phi_1]\\ -\partial_{\tau_1}p_1+\chi_1\nabla_\perp^2 p_1-[\phi_1,p_1]\end{pmatrix}. \tag{34}$$

We expand the solution of Eq.(34) into the Fourier series as in Eq.(24)

$$\begin{pmatrix}\phi_2\\ p_2\end{pmatrix}=\sum_{n=0}^{\infty}\begin{pmatrix}\phi_{0n}(x)\sin kn\Delta z\\ p_{0n}(x)\cos kn\Delta z\end{pmatrix}+\sum_{m=1}^{\infty}\sum_{n=-\infty}^{\infty}\begin{pmatrix}\phi_{mn}(x)\sin k(my+n\Delta z)\\ p_{mn}(x)\cos k(my+n\Delta z)\end{pmatrix}. \tag{35}$$

From Eqs.(34) and (35), we have for the $m=1$ modes

$$\mathbf{L}_{1n}\begin{pmatrix}\phi_{1n}(x)\\ p_{1n}(x)\end{pmatrix}=\begin{pmatrix}(\partial_{\tau_1}A_n)(\partial_x^2-k^2)\phi_1(x+n\Delta)-\chi_1 P_r A_n(\partial_x^2-k^2)^2\phi_1(x+n\Delta)\\ -(\partial_{\tau_1}A_n)p_1(x+n\Delta)+\chi_1 A_n(\partial_x^2-k^2)p_1(x+n\Delta)\end{pmatrix}. \tag{36}$$

The solvability condition for the $m=1$ mode equation (36) is given by

$$\left\langle\begin{pmatrix}\phi_1(x+n\Delta)\\ p_1(x+n\Delta)\end{pmatrix},\text{RHS of Eq.(36)}\right\rangle=\left\langle\mathbf{L}_{1n}\begin{pmatrix}\phi_1(x+n\Delta)\\ p_1(x+n\Delta)\end{pmatrix},\begin{pmatrix}\phi_{1n}(x+n\Delta)\\ p_{1n}(x+n\Delta)\end{pmatrix}\right\rangle=0 \tag{37}$$

where Eqs.(32), (33) and (36) are used. Equation (37) reduces to

$$\begin{aligned}&\int_{-\infty}^{\infty}dx\,[\,(\partial_{\tau_1}A_n)\{|\partial_x\phi_1(x+n\Delta)|^2+k^2\phi_1^2(x+n\Delta)+p_1^2(x+n\Delta)\}\\&\quad+\chi_1 A_n\{P_r|(\partial_x^2-k^2)\phi_1(x+n\Delta)|^2+|\partial_x p_1(x+n\Delta)|^2+k^2p_1^2(x+n\Delta)\}\,]\\&=0.\end{aligned} \tag{38}$$

Since an arbitrariness remains in the perturbation method given by Eq.(25), we can impose an additional constraint. If we assume that $\chi_1=0$ (or $\partial_{\tau_1}A_n=0$), we have

$$\chi_1=\partial_{\tau_1}A_n=0. \tag{39}$$

Then Eq.(36) has the same form as Eq.(33) so that the solution is given by $(\phi_{1n}(x),p_{1n}(x))^T=$ const. $\cdot\,(\phi_1(x+n\Delta),p_1(x+n\Delta))^T$. *Including this into the* $O(\lambda)$ *solution* makes it possible to put

$$\begin{pmatrix}\phi_{1n}(x)\\ p_{1n}(x)\end{pmatrix}=0. \tag{40}$$

For the $m = 0$, $n = 0$ mode,

$$\mathbf{L}_{00}\begin{pmatrix}\phi_{00}(x)\\ p_{00}(x)\end{pmatrix} \equiv \begin{pmatrix}\chi_c P_r \partial_x^4 \phi_{00}(x)\\ -\chi_c \partial_x^2 p_{00}(x)\end{pmatrix} = \begin{pmatrix}0\\ \frac{1}{2}k\sum_{n=-\infty}^{\infty} A_n^2 \partial_x\{\phi_1(x+n\Delta)p_1(x+n\Delta)\}\end{pmatrix}. \tag{41}$$

For the $m = 0$, $n \geq 1$ mode,

$$\mathbf{L}_{0n}\begin{pmatrix}\phi_{0n}(x)\\ p_{0n}(x)\end{pmatrix} = \frac{1}{2}k\sum_{n_1-n_2=n} A_{n_1}A_{n_2}\begin{pmatrix}\partial_x\{\phi_1(x+n_1\Delta)\partial_x^2\phi_1(x+n_2\Delta) - \phi_1(x+n_2\Delta)\partial_x^2\phi_1(x+n_1\Delta)\}\\ \partial_x\{\phi_1(x+n_1\Delta)p_1(x+n_2\Delta) + \phi_1(x+n_2\Delta)p_1(x+n_1\Delta)\}\end{pmatrix}. \tag{42}$$

For the $m = 2$ mode

$$\mathbf{L}_{2n}\begin{pmatrix}\phi_{2n}(x)\\ p_{2n}(x)\end{pmatrix} = \frac{1}{2}k\sum_{n_1+n_2=n} A_{n_1}A_{n_2}\begin{pmatrix}\partial_x\phi_1(x+n_1\Delta)\partial_x^2\phi_1(x+n_2\Delta) - \phi_1(x+n_1\Delta)\partial_x^3\phi_1(x+n_2\Delta)\\ -\partial_x\phi_1(x+n_1\Delta)p_1(x+n_2\Delta) + \phi_1(x+n_1\Delta)\partial_x p_1(x+n_2\Delta)\end{pmatrix}. \tag{43}$$

For the $m \geq 3$ mode, we have $\mathbf{L}_{mn}\left(\phi_{mn}(x), p_{mn}(x)\right)^T = 0$ which gives

$$\begin{pmatrix}\phi_{mn}(x)\\ p_{mn}(x)\end{pmatrix} = 0. \tag{44}$$

Thus the fluctuations in $O(\lambda^2)$ consist of the $m = 0$ and $m = 2$ modes which are obtained from the $m = 1$ modes in $O(\lambda)$ by Eqs.(4.41)-(4.43).

We have the equations in $0(\lambda^3)$ from Eqs.(5) and (6)

$$\mathbf{L}\begin{pmatrix}\phi_3\\ p_3\end{pmatrix} = \begin{pmatrix}\partial_{r_2}\nabla_1^2\phi_1 - \chi_2 P_r \nabla_1^4\phi_1 + [\phi_1, \nabla_1^2\phi_2] + [\phi_2, \nabla_1^2\phi_1]\\ -\partial_{r_2}p_1 + \chi_2\nabla_1^2 p_1 - [\phi_1, p_2] - [\phi_2, p_1]\end{pmatrix}. \tag{45}$$

If the Fourier expansion is done for $(\phi_3, p_3)^T$ as in Eq.(35), we obtain for the $m = 1$ modes

$$\mathbf{L}_{1n}\begin{pmatrix}\phi_{1n}^{(3)}(x)\\ p_{1n}^{(3)}(x)\end{pmatrix}$$

$$= \begin{pmatrix} (\partial_{\tau_2} A_n)(\partial_x^2 - k^2)\phi_1(x + n\Delta) - \lambda_2 P_r A_n(\partial_x^2 - k^2)^2\phi_1(x + n\Delta) + [\phi_1, \nabla_\perp^2\phi_2]_{1n} + [\phi_2, \nabla_\perp^2\phi_1]_{1n} \\ -(\partial_{\tau_2} A_n)p_1(x + n\Delta) + \lambda_2 A_n(\partial_x^2 - k^2)p_1(x + n\Delta) - [\phi_1, p_2]_{1n} - [\phi_2, p_1]_{1n} \end{pmatrix} \tag{46}$$

where $(\phi_{1n}^{(3)}(x), p_{1n}^{(3)}(x))^T$ denotes the $m = 1, n = n$ Fourier mode of $(\phi^{(3)}, p^{(3)})^T$ and

$$\begin{aligned}
&[\phi_1, \nabla_\perp^2\phi_2]_{1n} \\
= \; & -\frac{1}{4}k^2 \sum_{n_1=1}^{\infty}\sum_{n_2=-\infty}^{\infty} A_{n-n_1}A_{n_1+n_2}A_{n_2}\phi_1(x + (n - n_1)\Delta)\partial_x^3 F_{n_1}(x + n_2\Delta) \\
& +\frac{1}{4}k^2 \sum_{n_1=1}^{\infty}\sum_{n_2=-\infty}^{\infty} A_{n+n_1}A_{n_1+n_2}A_{n_2}\phi_1(x + (n + n_1)\Delta)\partial_x^3 F_{n_1}(x + n_2\Delta) \\
& -\frac{1}{4}k^2 \sum_{n_1=-\infty}^{\infty}\sum_{n_2=-\infty}^{\infty} A_{n_1-n}A_{n_1-n_2}A_{n_2}\{2\partial_x\phi_1(x + (n_1 - n)\Delta)(\partial_x^2 - 4k^2)H_{n_1-2n_2}(x + n_2\Delta) \\
& \qquad +\phi_1(x + (n_1 - n)\Delta)(\partial_x^3 - 4k^2\partial_x)H_{n_1-2n_2}(x + n_2\Delta)\} \\
&[\phi_2, \nabla_\perp^2\phi_1]_{1n} \\
= \; & \frac{1}{4}k^2 \sum_{n_1=1}^{\infty}\sum_{n_2=-\infty}^{\infty} A_{n-n_1}A_{n_1+n_2}A_{n_2}(\partial_x^2 - k^2)\phi_1(x + (n - n_1)\Delta)\partial_x F_{n_1}(x + n_2\Delta) \\
& -\frac{1}{4}k^2 \sum_{n_1=1}^{\infty}\sum_{n_2=-\infty}^{\infty} A_{n+n_1}A_{n_1+n_2}A_{n_2}(\partial_x^2 - k^2)\phi_1(x + (n + n_1)\Delta)\partial_x F_{n_1}(x + n_2\Delta) \\
& +\frac{1}{4}k^2 \sum_{n_1=-\infty}^{\infty}\sum_{n_2=-\infty}^{\infty} A_{n_1-n}A_{n_1-n_2}A_{n_2}\{2(\partial_x^3 - k^2\partial_x)\phi_1(x + (n_1 - n)\Delta)H_{n_1-2n_2}(x + n_2\Delta) \\
& \qquad +(\partial_x^2 - k^2)\phi_1(x + (n_1 - n)\Delta)\partial_x H_{n_1-2n_2}(x + n_2\Delta)\} \\
&[\phi_1, p_2]_{1n} \\
= \; & -\frac{1}{4}k^2 \sum_{n_1=0}^{\infty}\sum_{n_2=-\infty}^{\infty} A_{n-n_1}A_{n_1+n_2}A_{n_2}\phi_1(x + (n - n_1)\Delta)\partial_x G_{n_1}(x + n_2\Delta) \\
& -\frac{1}{4}k^2 \sum_{n_1=0}^{\infty}\sum_{n_2=-\infty}^{\infty} A_{n+n_1}A_{n_1+n_2}A_{n_2}\phi_1(x + (n + n_1)\Delta)\partial_x G_{n_1}(x + n_2\Delta) \\
& -\frac{1}{4}k^2 \sum_{n_1=-\infty}^{\infty}\sum_{n_2=-\infty}^{\infty} A_{n_1-n}A_{n_1-n_2}A_{n_2}\{2\partial_x\phi_1(x + (n_1 - n)\Delta)I_{n_1-2n_2}(x + n_2\Delta) \\
& \qquad +\phi_1(x + (n_1 - n)\Delta)\partial_x I_{n_1-2n_2}(x + n_2\Delta)\} \\
&[\phi_2, p_1]_{1n} \\
= \; & \frac{1}{4}k^2 \sum_{n_1=1}^{\infty}\sum_{n_2=-\infty}^{\infty} A_{n-n_1}A_{n_1+n_2}A_{n_2}p_1(x + (n - n_1)\Delta)\partial_x F_{n_1}(x + n_2\Delta) \\
& -\frac{1}{4}k^2 \sum_{n_1=1}^{\infty}\sum_{n_2=-\infty}^{\infty} A_{n+n_1}A_{n_1+n_2}A_{n_2}p_1(x + (n + n_1)\Delta)\partial_x F_{n_1}(x + n_2\Delta)
\end{aligned}$$

$$-\frac{1}{4}k^2\sum_{n_1=-\infty}^{\infty}\sum_{n_2=-\infty}^{\infty}A_{n_1-n}A_{n_1-n_2}A_{n_2}\{2\partial_x p_1(x+(n_1-n)\Delta)H_{n_1-2n_2}(x+n_2\Delta)$$
$$+p_1(x+(n_1-n)\Delta)\partial_x H_{n_1-2n_2}(x+n_2\Delta)\}.$$

Here F_n, G_n, H_n and I_n are given by

$$\mathbf{L}_{0n}\begin{pmatrix}F_n(x)\\G_n(x)\end{pmatrix} = \begin{pmatrix}\partial_x\{\phi_1(x+n\Delta)\partial_x^2\phi_1(x)-\phi_1(x)\partial_x^2\phi_1(x+n\Delta)\}\\ \partial_x\{\phi_1(x+n\Delta)p_1(x)+\phi_1(x)p_1(x+n\Delta)\}\end{pmatrix}$$

$$\mathbf{L}_{2n}\begin{pmatrix}H_n(x)\\I_n(x)\end{pmatrix} = \begin{pmatrix}\partial_x\phi_1(x+n\Delta)\partial_x^2\phi_1(x)-\phi_1(x+n\Delta)\partial_x^3\phi_1(x)\\ -\partial_x\phi_1(x+n\Delta)p_1(x)+\phi_1(x+n\Delta)\partial_x p_1(x)\end{pmatrix}$$

$$-\chi_c\partial_x^2 G_0(x) = \partial_x\{\phi_1(x)p_1(x)\}.$$

In the same manner as in Eq.(37), the solvability condition of Eq.(46) is given by

$$\left\langle\begin{pmatrix}\phi_1(x+n\Delta)\\ p_1(x+n\Delta)\end{pmatrix}, \text{RHS of Eq.(46)}\right\rangle = 0 \tag{47}$$

which reduces to

$$D_0\frac{\partial A_n}{\partial\tau_2}+\chi_2 D_1 A_n+\sum_{n_1,n_2}D_{n-n_2,n-n_1}A_{n-n_1+n_2}A_{n_1}A_{n_2}=0. \tag{48}$$

Rewriting

$$\lambda A_n\to A_n,\qquad \tau_2\to\lambda^2 t,\qquad \lambda^2\chi_2\to(\chi-\chi_c) \tag{49}$$

yields

$$D_0\frac{\partial A_n}{\partial t}+(\chi-\chi_c)D_1A_n+\sum_{n_1,n_2}D_{n-n_2,n-n_1}A_{n-n_1+n_2}A_{n_1}A_{n_2}=0 \tag{50}$$

where

$$D_0=\int_{-\infty}^{\infty}dx[|\partial_x\phi_1(x)|^2+k^2\phi_1^2(x)+p_1^2(x)] \tag{51}$$

$$D_1=\int_{-\infty}^{\infty}dx[P_r|(\partial_x^2-k^2)\phi_1(x)|^2+|\partial_x p_1(x)|^2+k^2p_1^2(x)] \tag{52}$$

$$\sum_{n_1,n_2}D_{n-n_1,n-n_2}A_{n-n_1+n_2}A_{n_1}A_{n_2}$$
$$=\int_{-\infty}^{\infty}dx[-\phi_1(x+n\Delta)\{[\phi_1,\nabla_\perp^2\phi_2]_{1n}+[\phi_2,\nabla_\perp^2\phi_1]_{1n}\}$$
$$+p_1(x+n\Delta)\{[\phi_1,p_2]_{1n}+[\phi_2,p_1]_{1n}\}]. \tag{53}$$

Equation (50) determines the behavior of the amplitude A_n in the solution of the leading order (27) near the marginally stable state.

V. COMPARISON BETWEEN THEORY AND NUMERICAL SIMULATIONS OF SYMMETRIC SOLUTION

In this section the results of the weakly nonlinear theory in the previous section are compared with those of the numerical simulations of Eqs.(5) and (6). Here we consider the symmetric solutions which are invariant under the transformations **T** and **P** given in Section III

$$\mathbf{T\Phi} = \mathbf{P\Phi} = \mathbf{\Phi}. \tag{54}$$

Then it follows that $A_n = A \quad (n = 0, \pm 1, \pm 2, \cdots)$ and Eq.(50) reduces to the following Landau equation:

$$D_0 \partial_t A + (\chi - \chi_c) D_1 A + D_3 A^3 = 0 \tag{55}$$

where

$$\begin{aligned}
D_3 \;=\; & \frac{1}{2} k \int_{-\infty}^{\infty} dx [-p_1(x) \sum_{n=0}^{\infty} \{\phi_1(x - n\Delta) + \phi_1(x + n\Delta) \partial_x p_{0n}(x) \\
& - p_1(x) \sum_{n=-\infty}^{\infty} \{2\partial_x \phi_1(x + n\Delta) \cdot p_{2n}(x) + \phi_1(x + n\Delta) \partial_x p_{2n}(x)\} \\
& + p_1(x) \sum_{n=1}^{\infty} \{p_1(x - n\Delta) - p_1(x + n\Delta)\} \partial_x \phi_{0n}(x) \\
& - p_1(x) \sum_{n=-\infty}^{\infty} \{2\partial_x p_1(x + n\Delta) \cdot \phi_{2n}(x) + p_1(x + n\Delta) \partial_x \phi_{2n}(x)\} \\
& + \phi_1(x) \sum_{n=1}^{\infty} \{\phi_1(x - n\Delta) - \phi_1(x + n\Delta)\} \partial_x^3 \phi_{0n}(x) \\
& + \phi_1(x) \sum_{n=-\infty}^{\infty} \{2\partial_x \phi_1(x + n\Delta) \cdot (\partial_x^2 - (2k)^2) \phi_{2n}(x) \\
& \qquad + \phi_1(x + n\Delta)(\partial_x^3 - (2k)^2 \partial_x) \phi_{2n}(x)\} \\
& - \phi_1(x) \sum_{n=1}^{\infty} (\partial_x^2 - k^2) \{\phi_1(x - n\Delta) - \phi_1(x + n\Delta)\} \cdot \partial_x \phi_{0n}(x) \\
& - \phi_1(x) \sum_{n=-\infty}^{\infty} \{2(\partial_x^3 - k^2 \partial_x) \phi_1(x + n\Delta) \cdot \partial_x \phi_{2n}(x) \\
& \qquad + (\partial_x^2 - k^2) \phi_1(x + n\Delta) \cdot \partial_x \phi_{2n}(x)\}].
\end{aligned} \tag{56}$$

The solution of the Landau equation is easily obtained and written as

$$A^2 = \frac{A_\infty^2}{1 + (A_\infty^2/A_0^2 - 1)\exp(-2\sigma t)} \tag{57}$$

where $A_0 = A(t = 0)$ and

$$\sigma = (\chi_c - \chi)D_1/D_0 \tag{58}$$

$$A_\infty^2 = (\chi_c - \chi)D_1/D_3. \tag{59}$$

Equations (51) and (52) show that $D_0 > 0$ and $D_3 > 0$. We find from Eqs.(57) and (58) that if $\chi > \chi_c$ then $\sigma < 0$ and $A \sim A_0 \exp(\sigma t)$, i.e., the linear theory holds as $t \to \infty$ for sufficiently small A_0. As will be found in the detailed calculations, D_3 is positive in the cases treated here. In the case of $\chi < \chi_c$, we have $\sigma > 0$ and $A \sim A_0 \exp(\sigma t)$ as $t \to -\infty$ for sufficiently small A_0. In this case, $A \to A_\infty$ as $t \to \infty$ for arbitrary magnitudes of A_0. The volume-averaged convective flux $\langle pv_x \rangle$, in which the contributions from the $m = 1$ modes are dominant, is $O(\lambda^2)$ and given by

$$\begin{aligned}
\langle pv_x \rangle &= -\langle p\partial_y \phi \rangle \\
&= -\frac{kA^2}{2\Delta} \sum_{n=-\infty}^{\infty} \int_0^\Delta dx p_1(x + n\Delta)\phi_1(x + n\Delta) \\
&= -\frac{kA^2}{2\Delta} \int_{-\infty}^{\infty} dx p_1(x)\phi_1(x).
\end{aligned} \tag{60}$$

Equations (59) and (60) yield the volume-averaged convective flux in the stationary state

$$\langle pv_x \rangle_\infty = -(\chi_c - \chi)\frac{k}{2\Delta}\frac{D_1}{D_3} \int_{-\infty}^{\infty} dx p_1(x)\phi_1(x). \tag{61}$$

In the right-hand side of Eq.(61), the calculation of D_3 is most complicated as seen in Eq.(56). It is found from the numerical calculations that the most dominant contribution to D_3 is from the terms relating to the pressure gradient of the $(m = 0, n = 0)$ mode $\partial_x p_{00}(x)$. From Eq.(41), we have

$$\partial_x p_{00}(x) = -\frac{k}{2\chi_c} \left\{ \sum_{n=-\infty}^{\infty} \phi_1(x + n\Delta)p_1(x + n\Delta) - C_0 \right\} \tag{62}$$

where the integral constant C_0 is determined by the condition that the volume average of $\partial_x p_{00}(x)$ vanishes and is given by

$$C_0 = \frac{1}{\Delta} \sum_{n=-\infty}^{\infty} \int_0^\Delta dx \phi_1(x + n\Delta)p_1(x + n\Delta) = \frac{1}{\Delta} \int_{-\infty}^{\infty} dx \phi_1(x)p_1(x) \tag{63}$$

The contribution from the terms shown by Eq.(62) to D_3 is represented by $D_3^{(0)}$:

$$\begin{aligned} D_3^{(0)} &= k\int_{-\infty}^{\infty} dx\{-p_1(x)\phi_1(x)\partial_x p_{00}(x)\} \\ &= \frac{k^2}{2\chi_c}\int_{-\infty}^{\infty} dx p_1(x)\phi_1(x)\left\{\sum_{n=-\infty}^{\infty}\phi_1(x+n\Delta)p_1(x+n\Delta) - C_0\right\} \\ &= \frac{k^2}{2\chi_c}\left[\int_{-\infty}^{\infty} dx p_1(x)\phi_1(x)\sum_{n=-\infty}^{\infty}\phi_1(x+n\Delta)p_1(x+n\Delta) - \Delta C_0^2\right] \\ &= \frac{k^2}{2\chi_c}\left[\int_0^{\Delta} dx\left\{\sum_{n=-\infty}^{\infty} p_1(x+n\Delta)\phi_1(x+n\Delta)\right\}^2 - \Delta C_0^2\right] \\ &= \frac{k^2}{2\chi_c}\int_0^{\Delta} dx\left\{\sum_{n=-\infty}^{\infty} p_1(x+n\Delta)\phi_1(x+n\Delta) - C_0\right\}^2 \end{aligned} \tag{64}$$

Equation (64) shows that $D_3^{(0)}$ is always positive and contributes to the saturation of the fluctuations. We find that $D_3^{(0)} \to +0$ as $\Delta \to +0$. Thus for sufficiently small Δ, the saturation mechanism due to $D_3^{(0)}$ is negligibly weak and if the other terms in D_3 are less effective the saturation amplitude becomes so large that the weakly nonlinear theory itself is supposed to give inaccurate results. When Δ is larger than the scale lengths of the $m = 1$ mode structures $\phi_1(x)$ and $p_1(x)$, Eq.(64) is approximated by

$$D_3^{(0)} \simeq \frac{k^2}{2\chi_c}\left[\int_{-\infty}^{\infty} dx\{p_1(x)\phi_1(x)\}^2 - \Delta^{-1}\left\{\int_{-\infty}^{\infty} dx p_1(x)\phi_1(x)\right\}^2\right] \tag{65}$$

Equation (65) shows that, also in this case, $D_3^{(0)}$ decreases and the saturation amplitude becomes larger as Δ decreases.

Figure 1 shows the time evolution of the convective flux $\langle pv_x\rangle$ for $\chi = 4.4 \times 10^{-1}$, $P_r = 1$, $k = 1$ and $\Delta = 5$. In this case the critical diffusivity for the $m = 1$ modes is $\chi_c = 4.771 \times 10^{-1}$. Here the thoretical result (a solid curve) obtained by Eqs.(57) (60) and the numerical result (solid circles) obtained by the simulations of Eqs.(5) and (6) are given. Both results are in good agreement. The units of the time t and the convective flux $\langle pv_x\rangle$ are obtained from Eq.(4). In the simulations of Eqs.(5) and (6), $\phi(x, y, z)$ and $p(x, y, z)$ are expanded into the Fourier modes as in Eq.(24) and we imposed the boundary conditions

$$\lim_{|x|\to\infty}\phi_{m,n}(x) = \lim_{|x|\to\infty} p_{m,n}(x) = 0 \qquad \text{for} \quad m \geq 1 \tag{66}$$

and the symmetry constraint (54) which gives

$$\phi_{m,n}(x) = \phi_{m,m+n}(x-\Delta) \tag{67}$$

$$p_{m,n}(x) = p_{m,m+n}(x-\Delta) \tag{68}$$

We find from Eqs.(66) and (67) that the $m=0$ mode structures $\phi_{0n}(x)$ and $p_{0n}(x)$ are the periodic functions of x with the period Δ

$$\phi_{0,n}(x+\Delta) = \phi_{0,n}(x), \qquad p_{0,n}(x+\Delta) = p_{0,n}(x). \tag{69}$$

Figures 2 show the electrostatic potential and the total pressure in the saturated state of the multiple-helicity resistive interchange mode obtained from the numerical simulation of Eqs.(5) and (6). Here $\chi = 4.4 \times 10^{-1}$, $P_r = 1$, $k = 1$ and $\Delta = 4$. In the numerical simulation we have included the modes with $0 \le m \le 5$. Figure 2(a) shows the contours of the electrostatic potential in the $x-y$ plane for $z=0$. In this case the $m=1$ mode structures appear dominantly, the profiles of which are shown in Fig.2(b). The $m=1$ mode structures are similar to those of the linear eigenfunctions obtained from Eq.(33) except that the former is somewhat broader than the latter due to the higher order nonlinear interaction. Figures 2(c) and (d) show the contours of the total pressure and the profile of that averaged in the y direction. We see the flattening of the pressure around the $m=1$ mode rational surfaces.

Figure 3 shows the dependence of the convective flux $\langle pv_x \rangle$ in the saturated state on the diffusivity χ obtained from the theoretical expression Eq.(61) and the simulations of Eqs.(5) and (6). Here $P_r = 1$, $k = 1$ and $\Delta = 5$. The theoretical results are in good agreement with the simulation results. For small χ the convective flux obtained from the simulations is smaller than that obtained from the theory due to the higher order nonlinear corrections.

Figure 4 shows the dependence of the saturated convective flux $\langle pv_x \rangle$ multiplied by Δ on Δ^{-1}. Here $P_r = 1$, $k = 1$ and $\chi = 4.4 \times 10^{-1}$. As seen from Eq.(60), $\langle pv_x \rangle \Delta = -\frac{1}{2} k A^2 \int_{-\infty}^{\infty} dx p_1(x)\phi_1(x)$ denotes the convection of a single $m=1$ mode integrated over $-\infty < x < \infty$. Since the values of k and χ are fixed here, the linear mode structures

remain unchanged and therefore Δ^{-1} represents the measure for the ratio of the width of the $m = 1$ mode structure to the interval between the neighboring $m = 1$ mode rational surfaces (or the extent to which the neighboring $m = 1$ modes overlap). Here the results of the theory [Eq(61)] and the simulations of Eqs.(5) and (6) are shown. We find from Eq.(61) that $\langle pv_x \rangle \Delta$ depends on Δ^{-1} only through D_3 in the denominator. The dependence of D_3 on Δ^{-1} is also shown. As Δ^{-1} is increased, D_3 is monotonically decreased and therefore $\langle pv_r \rangle \Delta$ is monotonically increased. For small Δ^{-1}, D_3 has the form of the first degree polynomial function of Δ^{-1} as predicted from Eq.(65). The simulation results are well described by the theoretical predictions but for larger Δ^{-1} the former show the more rapid increase of $\langle pv_x \rangle \Delta$ than the latter. Thus we see that the higher order nonlinear corrections enhance the saturation amplitude for larger Δ^{-1} while they lower that for smaller λ as seen from Fig.3.

VI. CONCLUSIONS AND DISCUSSION

In this paper we have generalized the weakly nonlinear theory for sigle-helicity modes of Hamaguchi and Nakajima to the case of multiple-helicity modes in the local sheared slab configuration. We have found that the model equations are invariant under the transformation $\mathbf{T}$ defined by Eq.(12) or (13) and that this invariance property holds generally for other local reduced fluid model equations in the slab geometry with constant magnetic shear. From this property it follows that there exist the multiple-helicity modes which correspond to the critical order parameter (in this paper we used the diffusivity as a order parameter but other quantities such as the pressure gradient or the average magnetic curvature can be used in the same way) or in other words that the critical order parameter is degenerate due to the multiple-helicity modes, which are produced by operating $\mathbf{T}$ successively. Then the weakly nonlinear theory for the multiple-helicity modes is quite naturally developed from the single-helicity case and we have obtained the governing equations (50) for the amplitudes $\{A_n\}$ of multiple-helicity resistive interchange modes near marginal stability.

We have compared the thoretical results with those obtained by the numerical simulation of the model equations for the cases of the symmetric solutions, in which all the amplitudes A_n of the dominant ($m = 1$) modes have the same value. We have seen that both results are in good agreement in the parameter region near the marginal stability. The symmetry conditions used here are suitable to the local transport problem since they are free from boundary layers with steep pressure gradients as is seen under fixed boundary conditions, which produce artificially distorted pressure profile inappropriate to the local model. In this condition the weakly nonlinear behavior of the multiple-helicity modes is described by the Landau equation (55) in the same way as in the single-helicity case. When the diffusivity χ becomes smaller than the critical value χ_c (which depends on the minimum wavenumber k and the Prandtl number P_r), the new stationary states with convective cells bifurcates from static equilibria. Then the convective transport or the effective pressure diffusivity defined by $\chi_{NL} = \langle pv_x \rangle / (-dP_0(x)/dx)$ is proportional to $(\chi_c - \chi)$. It was also shown that

when the ratio of the interval Δ between the $m = 1$ modes to the radial width of the mode profile decreases, the saturation amplitude per single mode becomes larger than that in the single-helicity case and the convective transport of the multi-helicity modes is more enhanced than that predicted by the linear superposition of the saturated convection of the single-helicity cases. Here only the symmetric solutions are examined but the nonlinear amplitude equations (50) may have other various types of solutions and it is interesting as a future task to investigate spatial patterns and nonliear stability of such solutions.

In the parameter range of actutual experimental devices plasmas are supposed to lie in the strong nonlinear or turbulent states, which are far from marginal stability. In order to estimate the turbulent diffusivity χ_{turb} in such strong nonlinear states, the following heuristic argument is often used. Replacing the nonlinear convection $v \cdot \nabla_\perp$ with the turbulent diffusion $-\chi_{turb}\nabla_\perp^2$ in the model equations, the nonlinear growth rate $\gamma_{NL}(k_y, \chi)$ is expressed in terms of the linea growth rate $\gamma_l(k_y, \chi)$ as

$$\gamma_{NL}(k_y, \chi) = \gamma_L(k_y, \chi + \chi_{turb}) \tag{70}$$

where $P_r \simeq 1$ is assumed. It is considered that the stationary state is realized when $\gamma_{NL}(k_y, \chi) \leq 0$ for all wavenumbers k_y. For example if we assume that $\gamma_{NL}(k_y) = \gamma_l(k_y) - \chi_{turb}k_\perp^2$ then we have a well-known expression of the turbulent diffusivity $\chi_{turb} = (\gamma_L/k_\perp^2)_{max}$ for the stationary state. From Eq.(70) we have more general expression

$$\chi_{turb} = [\chi_c(k_y)]_{max} - \chi \tag{71}$$

where $\chi_c(k_y)$ is defined by the diffusivity required to linearly stabilize the mode with the wavenumber k_y i.e. $\gamma_L(k_y, \chi_c) = 0$. In order to obtain the turbulent diffusivity of the resistive interchange modes Carreras et al.[10] used the one-point renormalization theory and applied essentially the same argument as above to the stationary turbulent states. It is interesting that the effective diffusivity of the convection obtained in this paper by the weakly nonlinear theory has the form similar to Eq.(71), i.e., $\chi_{NL} = K(\chi_c(k) - \chi)$ where $\chi_c(k \equiv (k_y)_{min}) = [\chi_c(k_y)]_{max}$ holds and the coefficient K depends on k, P_r and Δ. This analogy between the expressions of the nonlinear diffusivity is naturally understood by noting that the Landau equation (55) derived by the weakly nonlinear theory includes the

nonlinearity in the way that it is obtained from the linear equation by replacing χ with $\chi + \chi_A$ ($\chi_A \equiv (D_3/D_1)A^2$) and that the stationary solution is given by $\chi + \chi_A = \chi_c$, which is the same logic as leading to Eq.(71).

As an example let us estimate the nonlinear thermal diffusivity for experimental plasma of Heliotron E, of which in the peripheral region the resitive interchange modes are unstable and supposed to cause the anomalous tranport. As local plasma parameters in the peripheral region of Heliotron E we use $n_e = n_i = 5 \times 10^{18} m^{-3}$, $T_e = T_i = 40eV$, $B = 1T$, $L_s = 0.6m$, $d\Omega/dr = 4.5m^{-1}$ and $L_p = |d\ln P_0/dr|^{-1} = 3 \times 10^{-2}m$. Then we have the collisional diffusivity $\chi = 6.1 \times 10^{-3} m^2/s$. We consider the local transport around the radial position of $r = 0.18m$ close to which there are no mode rational surfaces with low poloidal modenumbers $m_p = 1, 2, \cdots$ and we use $k_y = 5.9 \times 10^1 m^{-1}$ as the minimum wavenumber in the poloidal direction which corresponds to the poloidal modenumber $m_p = 10$. For that poloidal wavenumber the critical diffusivity is $\chi_c = 0.51 m^2/s$, the radial interval between the modes is given by $\Delta = 5 \times 10^{-3} m$ and the radial mode structure of the form $\phi \propto \exp[-\frac{1}{2}\{(x - x_s)/l_x\}^2]$ (where x_s denotes the radial position of the mode rational surface) with $l_x = 6 \times 10^{-4} m$ for which the significant effects of the neighboring mode interaction on the convective transport appear. From Eq.(61) we obtain the nonlinear pressure diffusivity $\chi_{NL} \equiv \langle p v_x \rangle / (-dP_0/dx) = K(\chi_c - \chi) = 1.0 m^2/s$ ($K = 2.0$). Using the relations $\frac{3}{2}\langle p v_x \rangle = -n\chi_{th} dT/dx$ and $d\ln P/dx = \Gamma/(\Gamma - 1) d\ln T/dx$ ($\Gamma = \frac{5}{3}$) we have the nonlinear thermal diffusivity $\chi_{th} = \frac{15}{4}\chi_{NL} \simeq 3.8 m^2/s$. This gives a reasonable value of the anomalous transport coefficient compared to the experimental values in Heliotron E[13] $\chi_{exp} = 1 \sim 10 m^2/s$ although more accurate estimation of anomalous transport and fluctuation spectra require the theory treating strong nonlinearity and high degree of freedom in the turbulent system. Since direct numerical simulations of three-dimensional stationary turbulence in experimental plasmas with such parameters as above require huge sizes of computer memory and time, further development of nonlinear theory to complement numerical simulation is indispensable.

ACKNOWLEDGEMENTS

The authors thank Professor Okamoto for his encouragements of this work. The numerical simulation was done on the computer at the National Institute for Fusion Science.

REFERENCES

1) P. C. Liewer, Nucl. Fusion **25**, 543 (1985).

2) P. G. Drazin and W. H. Reid, *Hydrodynamic Stability* (Cambridge U. P., Cambridge, 1981)

3) L. D. Landau and E. M. Lifshitz, *Fluid Mechanics* (Pergamon P., London, 1959)

4) E. Palm, J. Fluid Mech. **8**, 183 (1960).

5) W. V. R. Malkus and G. Veronis, J. Fluid Mech. **4**, 225 (1958).

6) S. Hamaguchi, Phys. Fluids B **1**, 1416 (1989).

7) N. Nakajima, Phys. Fluids B **2**, 1170 (1990).

8) N. Nakajima and S. Hamaguchi, Phys. Fluids B **2** 1184 (1990).

9) Y. C. Lee and J. W. Van Dam, in *Finite Beta Theory Workshop*, Varenna, 1977 (U. S. Department of Energy, Washington, DC, 1977), CONF-7709167, p.93

10) B. A. Carreras, L. Garcia, and P. H. Diamond, Phys. Fluids **30**, 1388 (1987).

11) G. S. Lee and B. A. Carreras, Phys. Fluids B **1**, 119 (1989).

12) H. Sugama and M. Wakatani, J. Phys. Soc. Jpn. **57**, 2010 (1988).

13) H. Zushi, T. Mizuuchi, O. Motojima, M. Wakatani, F. Sano, M. Sato, A. Iiyoshi, and K. Uo, Nucl. Fusion **28**, 433 (1988).

14) H. R. Strauss, Plasma Phys. **22**, 733 (1980).

15) H. Sugama and M. Wakatani, J. Phys. Soc. Jpn. **58**, 3859 (1989).

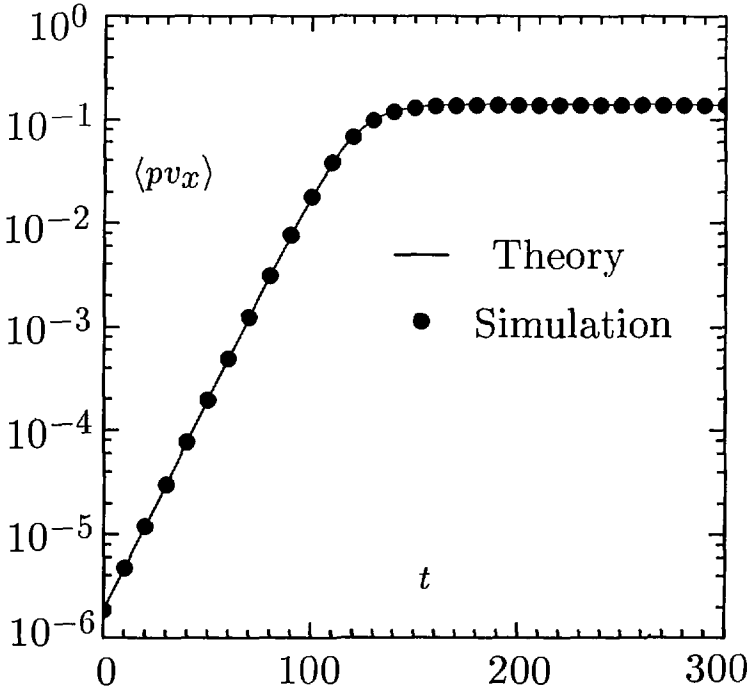

Fig.1 Time evolution of the convective flux $\langle pv_x \rangle$ for $\chi = 4.4 \times 10^{-1}$, $P_r = 1$, $k = 1$ and $\Delta = 5$. Theoretical and numerical results are shown by a solid curve and solid circles, respectively.

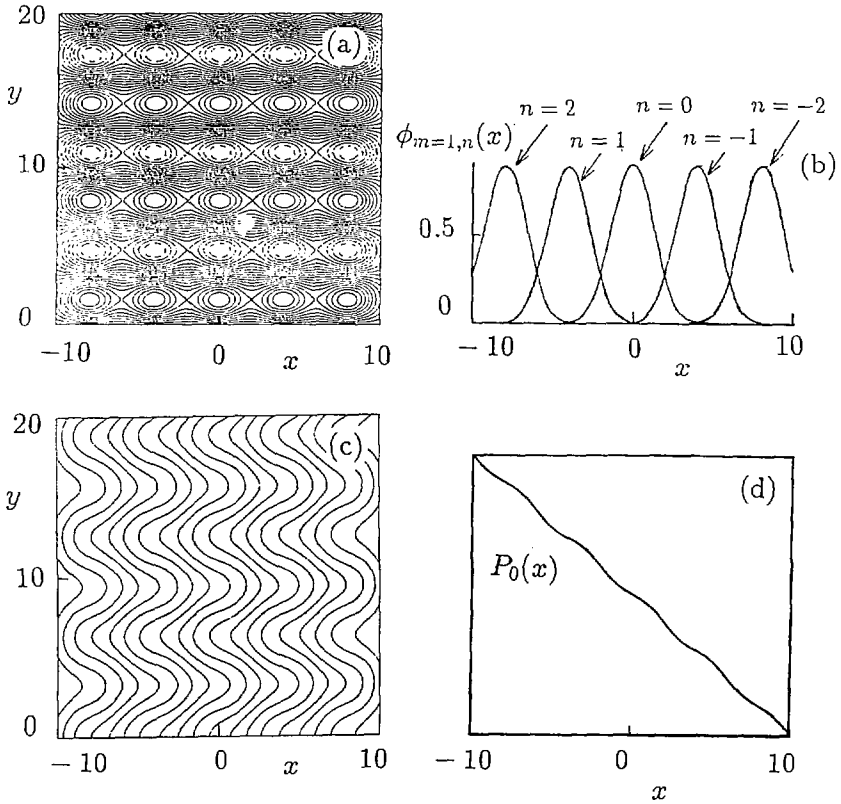

Fig.2 The electrostatic potential and the total pressure in the saturated state of the multiple-helicity resistive interchange modes obtained from the numerical simulation. Here $\chi = 4.4 \times 10^{-1}$, $P_r = 1$, $k = 1$ and $\Delta = 4$.

(a) The contours of the electrostatic potential in the $x - y$ plane for $z = 0$.

(b) The $m = 1$ mode structures of the electrostatic potential.

(c) The contours of the total pressure.

(d) The profile of the total pressure averaged in the y direction.

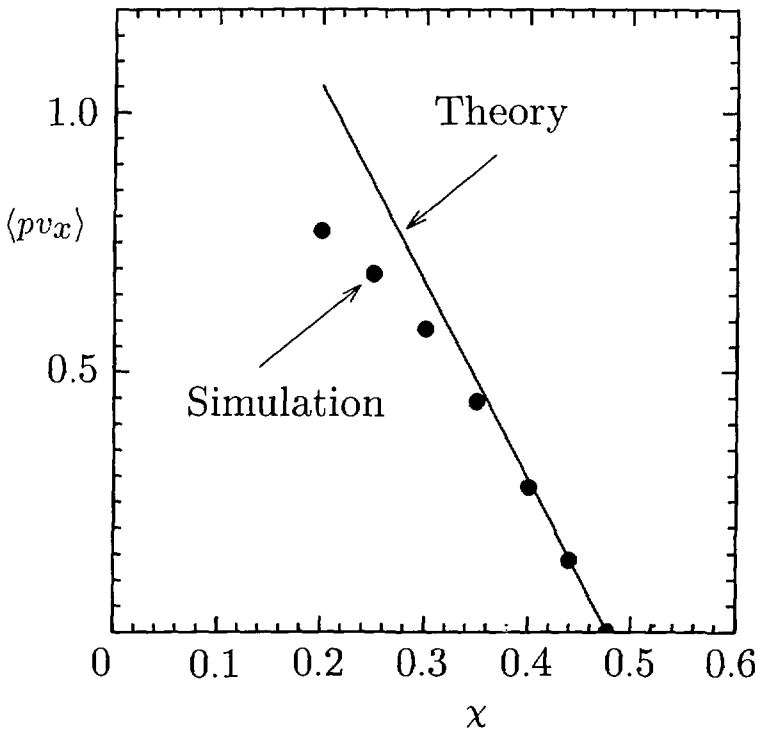

Fig.3 The saturated convective flux $\langle pv_x \rangle$ as a function of χ obtained from the theory and the simulations. Here $P_r = 1$, $k = 1$ and $\Delta = 5$.

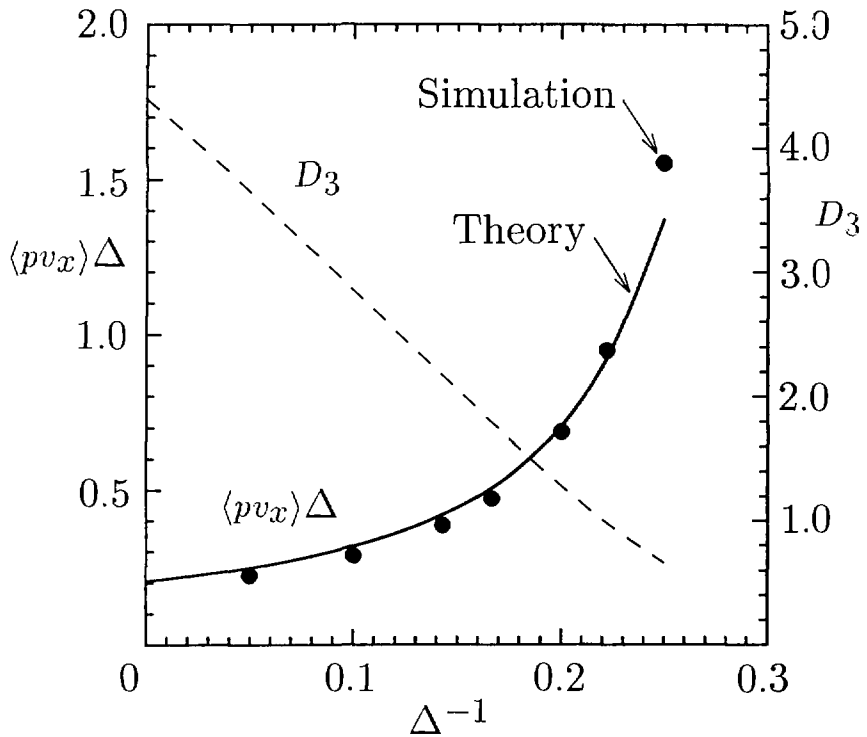

Fig.4 The saturated convective flux $\langle pv_x \rangle$ multiplied by Δ as a function of Δ^{-1} obtained from the theory and the simulations. The values of D_3 in the Landau equation is also shown. Here $P_r = 1$, $k = 1$ and $\chi = 4.4 \times 10^{-1}$.

Recen Issues of NIFS Series

NIFS-39 O. Kaneko, S. Kubo, K. Nishimura, T. Syoji, M. Hosokawa, K. Ida, H. Idei, H. Iguchi, K. Matsuoka, S. Morita, N. Noda, S. Okamura, T. Ozaki, A. Sagara, H. Sanuki, C. Takahashi, Y. Takeiri, Y. Takita, K. Tsuzuki, H. Yamada, T. Amano, A. Ando, M. Fujiwara, K. Hanatani, A. Karita, T. Kohmoto, A. Komori, K. Masai, T. Morisaki, O. Motojima, N. Nakajima, Y. Oka, M. Okamoto, S. Sobhanian and J. Todoroki, *Confinement Characteristics of High Power Heated Plasma in CHS*; Sep. 1990

NIFS-40 K. Toi, Y. Hamada, K. Kawahata, T. Watari, A. Ando, K. Ida, S. Morita, R. Kumazawa, Y. Oka, K. Masai, M. Sakamoto, K. Adati, R. Akiyama, S. Hidekuma, S. Hirokura, O. Kaneko, A. Karita, T. Kawamoto, Y. Kawasumi, M. Kojima, T. Kuroda, K. Narihara, Y. Ogawa, K. Ohkubo, S. Okajima, T. Ozaki, M. Sasao, K. Sato, K.N. Sato, T. Seki, F. Shimpo, H. Takahashi, S. Tanahashi, Y. Taniguchi and T. Tsuzuki, *Study of Limiter H- and IOC- Modes by Control of Edge Magnetic Shear and Gas Puffing in the JIPP T-IIU Tokamak*; Sep. 1990

NIFS-41 K. Ida, K. Itoh, S.-I. Itoh, S. Hidekuma and JIPP T-IIU & CHS Group, *Comparison of Toroidal/Poloidal Rotation in CHS Heliotron/Torsatron and JIPP T-IIU Tokamak*; Sep .1990

NIFS-42 T.Watari, R.Kumazawa,T.Seki, A.Ando,Y.Oka, O.Kaneko, K.Adati, R.Ando, T.Aoki, R.Akiyama, Y.Hamada, S.Hidekuma, S.Hirokura, E.Kako, A.Karita, K.Kawahata, T.Kawamoto, Y.Kawasumi, S.Kitagawa, Y.Kitoh, M.Kojima, T. Kuroda, K.Masai, S.Morita, K.Narihara, Y.Ogawa, K.Ohkubo, S.Okajima, T.Ozaki, M.Sakamoto, M.Sasao, K.Sato, K.N.Sato, F.Shinbo, H.Takahashi, S.Tanahashi, Y.Taniguchi, K.Toi, T.Tsuzuki, Y.Takase, K.Yoshioka, S.Kinoshita, M.Abe, H.Fukumoto, K.Takeuchi, T.Okazaki and M.Ohtuka, *Application of Intermediate Frequency Range Fast Wave to JIPP T-IIU and HT-2 Plasma*; Sep. 1990

NIFS-43 K.Yamazaki, N.Ohyabu, M.Okamoto, T.Amano, J.Todoroki, Y.Ogawa, N.Nakajima, H.Akao, M.Asao, J.Fujita, Y.Hamada, T.Hayashi, T.Kamimura, H.Kaneko, T.Kuroda, S.Morimoto, N.Noda, T.Obiki, H.Sanuki, T.Sato, T.Satow, M.Wakatani, T.Watanabe, J.Yamamoto, O.Motojima, M.Fujiwara, A.Iiyoshi and LHD Design Group, *Physics Studies on Helical Confinement Configurations with l=2 Continuous Coil Systems*; Sep. 1990

NIFS-44 T.Hayashi, A.Takei, N.Ohyabu, T.Sato, M.Wakatani, H.Sugama, M.Yagi, K.Watanabe, B.G.Hong and W.Horton, *Equilibrium Beta Limit and Anomalous Transport Studies of Helical Systems*; Sep. 1990

NIFS-45 R.Horiuchi, T.Sato, and M.Tanaka, *Three-Dimensional Particle Simulation Study on Stabilization of the FRC Tilting Instability*; Sep. 1990

NIFS-46 K.Kusano, T.Tamano and T. Sato, *Simulation Study of Nonlinear Dynamics in Reversed-Field Pinch Configuration*; Sep. 1990

NIFS-47 Yoshi H.Ichikawa, *Solitons and Chaos in Plasma*; Sep. 1990

NIFS-48 T.Seki, R.Kumazawa, Y.Takase, A.Fukuyama, T.Watari, A.Ando, Y.Oka, O.Kaneko, K.Adati, R.Akiyama, R.Ando, T.Aoki, Y.Hamada, S.Hidekuma, S.Hirokura, K.Ida, K.Itoh, S.-I.Itoh, E.Kako, A. Karita, K.Kawahata, T.Kawamoto, Y.Kawasumi, S.Kitagawa, Y.Kitoh, M.Kojima, T.Kuroda, K.Masai, S.Morita, K.Narihara, Y.Ogawa, K.Ohkubo, S.Okajima, T.Ozaki, M.Sakamoto, M.Sasao, K.Sato, K.N.Sato, F.Shinbo, H.Takahashi, S.Tanahashi, Y.Taniguchi, K.Toi and T.Tsuzuki, *Application of Intermediate Frequency Range Fast Wave to JIPP T-IIU Plasma*; Sep.1990

NIFS-49 A.Kageyama, K.Watanabe and T.Sato, *Global Simulation of the Magnetosphere with a Long Tail: The Formation and Ejection of Plasmoids*; Sep.1990

NIFS-50 S.Koide, *3-Dimensional Simulation of Dynamo Effect of Reversed Field Pinch*; Sep. 1990

NIFS-51 O.Motojima, K. Akaishi, M.Asao, K.Fujii, J.Fujita, T.Hino, Y.Hamada, H.Kaneko, S.Kitagawa, Y.Kubota, T.Kuroda, T.Mito, S.Morimoto, N.Noda, Y.Ogawa, I.Ohtake, N.Ohyabu, A.Sagara, T. Satow, K.Takahata, M.Takeo, S.Tanahashi, T.Tsuzuki, S.Yamada, J.Yamamoto, K.Yamazaki, N.Yanagi, H.Yonezu, M.Fujiwara, A.Iiyoshi and LHD Design Group, *Engineering Design Study of Superconducting Large Helical Device*; Sep. 1990

NIFS-52 T.Sato, R.Horiuchi, K. Watanabe, T. Hayashi and K.Kusano, *Self-Organizing Magnetohydrodynamic Plasma*; Sep. 1990

NIFS-53 M.Okamoto and N.Nakajima, *Bootstrap Currents in Stellarators and Tokamaks*; Sep. 1990

NIFS-54 K.Itoh and S.-I.Itoh, *Peaked-Density Profile Mode and Improved Confinement in Helical Systems*; Oct. 1990

NIFS-55 Y.Ueda, T.Enomoto and H.B.Stewart, *Chaotic Transients and Fractal Structures Governing Coupled Swing Dynamics*; Oct. 1990

NIFS-56 H.B.Stewart and Y.Ueda, *Catastrophes with Indeterminate Outcome*; Oct. 1990

NIFS-57 S.-I.Itoh, H.Maeda and Y.Miura, *Improved Modes and the Evaluation of Confinement Improvement*; Oct. 1990

NIFS-58 H.Maeda and S.-I.Itoh, *The Significance of Medium- or Small-size Devices in Fusion Research*; Oct. 1990

NIFS-59 A.Fukuyama, S.-I.Itoh, K.Itoh, K.Hamamatsu, V.S.Chan, S.C.Chiu, R.L.Miller and T.Ohkawa, *Nonresonant Current Drive by RF Helicity Injection*; Oct. 1990

NIFS-60 K.Ida, H.Yamada, H.Iguchi, S.Hidekuma, H.Sanuki, K.Yamazaki and CHS Group, *Electric Field Profile of CHS Heliotron/Torsatron Plasma with Tangential Neutral Beam Injection*; Oct. 1990

NIFS-61 T.Yabe and H.Hoshino, *Two- and Three-Dimensional Behavior of Rayleigh-Taylor and Kelvin-Helmholz Instabilities*; Oct. 1990

NIFS-62 H.B. Stewart, *Application of Fixed Point Theory to Chaotic Attractors of Forced Oscillators;* Nov. 1990

NIFS-63 K.Konn., M.Mituhashi, Yoshi H.Ichikawa,*Soliton on Thin Vortex Filament;* Dec. 1990

NIFS-64 K.Itoh, S.-I.Itoh and A.Fukuyama,*Impact of Improved Confinement on Fusion Research;* Dec. 1990

NIFS -65 A.Fukuyama, S.-I.Itoh and K. Itoh,*A Consistency Analysis on the Tokamak Reactor Plasmas;* Dec. 1990

NIFS-66 K.Itoh, H. Sanuki, S.-I. Itoh and K. Tani,*Effect of Radial Electric Field on α-Particle Loss in Tokamaks;* Dec. 1990

NIFS-67 K.Sato,and F.Miyawaki,*Effects of a Nonuniform Open Magnetic Field on the Plasma Presheath*; Jan.1991

NIFS-68 K.Itoh and S.-I.Itoh,*On Relation between Local Transport Coefficient and Global Confinement Scaling Law;* Jan. 1991

NIFS-69 T.Kato, K.Masai, T.Fujimoto,F.Koike, E.Källne, E.S.Marmar and J.E.Rice,*He-like Spectra Through Charge Exchange Processes in Tokamak Plasmas;* Jan.1991

NIFS-70 K. Ida, H. Yamada, H. Iguchi, K. Itoh and CHS Group, *Observation of Parallel Viscosity in the CHS Heliotron/Torsatron* ; Jan.1991

NIFS-71 H. Kaneko, *Spectral Analysis of the Heliotron Field with the Toroidal Harmonic Function in a Study of the Structure of Built-in Divertor* ; Jan. 1991

NIFS-72 S. -I. Itoh, H. Sanuki and K. Itoh, *Effect of Electric Field Inhomogeneities on Drift Wave Instabilities and Anomalous Transport* ; Jan. 1991

NIFS-73 Y.Nomura, Yoshi.H.Ichikawa and W.Horton, *Stabilities of Regular Motion in the Relativistic Standard Map*; Feb. 1991

NIFS-74 T.Yamagishi, *Electrostatic Drift Mode in Toroidal Plasma with Minority Energetic Particles*, Feb. 1991

NIFS-75 T.Yamagishi, *Effect of Energetic Particle Distribution on Bounce Resonance Excitation of the Ideal Ballooning Mode*, Feb. 1991

NIFS-76 T.Hayashi, A.Tadei, N.Ohyabu and T.Sato, *Suppression of Magnetic Surface Breading by Simple Extra Coils in Finite Beta Equilibrium of Helical System;* Feb. 1991

NIFS-77 N. Ohyabu, *High Temperature Divertor Plasma Operation*; Feb. 1991

NIFS-78 K.Kusano, T. Tamano and T. Sato, *Simulation Study of Toroidal Phase-Locking Mechanism in Reversed-Field Pinch Plasma*; Feb. 1991

NIFS-79 K. Nagasaki, K. Itoh and S. -I. Itoh, *Model of Divertor Biasing and Control of Scrape-off Layer and Divertor Plasmas*; Feb. 1991

NIFS-80 K. Nagasaki and K. Itoh, *Decay Process of a Magnetic Island by Forced Reconnection*; Mar. 1991

NIFS-81 K. Takahata, N. Yanagi, T. Mito, J. Yamamoto, O.Motojima and LHDDesign Group, K. Nakamoto, S. Mizukami, K. Kitamura, Y. Wachi, H. Shinohara, K. Yamamoto, M. Shibui, T. Uchida and K. Nakayama, *Design and Fabrication of Forced-Flow Coils as R&D Program for Large Helical Device*; Mar. 1991

NIFS-82 T. Aoki and T. Yabe, *Multi-dimensional Cubic Interpolation for ICF Hydrodynamics Simulation*; Apr. 1991

NIFS-83 K. Ida, S.-I. Itoh, K. Itoh and S. Hidekuma, *Density Peaking in the* May 1991

NIFS-84 A. Iiyoshi, *Development of the Stellarator/Heliotron Research*; May 1991

NIFS-85 Y. Okabe, M. Sasao, H. Yamaoka, M. Wada and J. Fujita, *Dependence of Au^- Production upon the Target Work Function in a Plasma-Sputter-Type Negative Ion Source;* May 1991

NIFS-86 N. Nakajima and M. Okamoto, *Geometrical Effects of the Magnetic Field on the Neoclassical Flow, Current and Rotation in General Toroidal Systems*; May 1991

NIFS-87 Sanae -I. Itoh, K. Itoh, A. Fukuyama, Y. Miura and JFT-2M Group, *ELMy-H mode as Limit Cycle and Chaotic oscillations in Tokamak Plasmas*, May 1991

NIFS-88 N. Matsunami and K. Kitoh ,*High Resolution Spectroscopy of H^+ Energy Loss in Thin Carbon Film;*May.1991